International Journal of Biological Macromolecules 244 (2023) 125478

Contents lists available at ScienceDirect

International Journal of Biological Macromolecules

journal homepage: www.elsevier.com/locate/ijbiomac

Thermoplastic starch/polyvinyl alcohol blends modification by citric acid–glycerol polyesters

Jennifer M. Castro [a,b], Mercedes G. Montalbán [c], Noelia Martínez-Pérez [a,b], Daniel Domene-López [a,b], Juana M. Pérez [d], Francisco M. Arrabal-Campos [d], Ignacio Fernández [d], Ignacio Martín-Gullón [a,b,*], Juan C. García-Quesada [a,b]

[a] Chemical Engineering Department, University of Alicante, Apartado 99, 03080 Alicante, Spain
[b] Institute of Chemical Process Engineering, University of Alicante, Apartado 99, 03080 Alicante, Spain
[c] Chemical Engineering Department, Faculty of Chemistry, Regional Campus of International Excellence "Campus Mare Nostrum", University of Murcia, 30071 Murcia, Spain
[d] Department of Chemistry and Physics, CIAIMBITAL Center, University of Almeria, 04120 Almeria, Spain

ARTICLE INFO

Keywords:
Thermoplastic starch/polyvinyl alcohol
Citric acid
Plasticizer

ABSTRACT

Thermoplastic starch/polyvinyl alcohol (TPS/PVA) films have limitations for being used in long–term applications due to starch retrogradation. This leads to plasticizer migration, especially when low molecular weight plasticizers such as glycerol, are used. In this work, we employed mixtures of oligomers based on glycerol citrates with higher molecular weight than glycerol as plasticizers for potato–based TPS/PVA blends obtained by melt–mixing. This constitutes an alternative to reduce plasticizer migration while keeping high swelling degree, and to provide high mechanical performance. The novelty lies in the usage of these oligomers by melt-mixing technique, aspect not deeply explored previously and that represents the first step towards industrial scalability. Prior to the blending process, oligomers mixtures were prepared with different molar ratios of citric acid (0–40 mol%) and added them. This minimizes the undesirable hydrolysis effect of free carboxylic groups on starch chains. The results demonstrated that the migration of plasticizers in TPS/PVA blends decreased by up to 70 % when the citric acid content increased. This reduction was attributed to the higher molecular weight (the majority in the range 764–2060 Da) and the 3D structure of the oligomers compared to using raw glycerol. Furthermore, the films exhibited a 150 % increase in Young's modulus and tensile strength without a reduction in elongation at break, while maintaining a high gel content, due to a moderate crosslinking.

1. Introduction

Biopolymers such as starch, cellulose or chitosan, are promising candidates to replace conventional polymers in certain packaging applications due to their abundance, low cost, and biodegradability [1,2]. Among all biopolymers, starch stands out as one of the most promising options. Unlike others, it can be easily converted thermoplastic starch (TPS) by gelatinization using standard thermoplastic processing equipment [3]. TPS exhibits desirable properties such as being odorless, tasteless, colorless, and non–toxic [4].

There are some main drawbacks associated with pure TPS films. Firstly, they exhibit poor mechanical performance, resulting in a brittle material, as plasticizer migration occurs, leading to fast aging [5]. Secondly, pure TPS films face challenges in consecutive transformation processing. To overcome these limitations, the blending of TPS with other biodegradable polymers such as polyvinyl alcohol (PVA), has been extensively studied in the literature [6–9]. PVA, the most widely produced biodegradable synthetic polymer worldwide, has been used in packaging materials due to its chemical resistance, good film–forming ability, oxygen barrier properties, compatibility with other materials, and excellent mechanical properties [4,10,11] Furthermore, PVA has been approved by the US Food and Drugs Administration (FDA) and the European Medicines Agency (EMA) for human use, making it safe for applications in food packaging [6]. TPS/PVA blends exhibit positive synergies, including improved strength and toughness compared to TPS and PVA individually [12,13], as well as a lower cost compared to using PVA alone. The chemical structure of PVA consists of hydrocarbon chains with polar hydroxyl groups (–OH), which can form

* Corresponding author at: Chemical Engineering Department, University of Alicante, Apartado 99, 03080 Alicante, Spain.
E-mail address: gullon@ua.es (I. Martín-Gullón).

https://doi.org/10.1016/j.ijbiomac.2023.125478
Received 26 April 2023; Received in revised form 13 June 2023; Accepted 16 June 2023
Available online 17 June 2023

intermolecular hydrogen bonds with starch facilitating better blending [14]. However, the presence of a plasticizer is necessary to gelatinize starch with PVA Traditionally, water has been used as plasticizer, but its limited processability window (below 100 °C) restricts the properties of starch/PVA films [15]. Therefore, water is commonly used with other plasticizers containing hydroxyl groups, such as glycerol [16,17], which can interact with starch and PVA molecules.

Starch retrogradation serves as the primary driving force behind plasticizer migration and the subsequent aging of TPS films. Slowing down this process has been a major objective over the last two decades. Migration leads to alterations in mechanical properties and crystallinity, involving the reorganization of gelatinized starch chains and resulting in unstable samples. Consequently, TPS films often have limitations for long–term applications. Plasticizer migration is usually favored by low molecular weight plasticizers such as glycerol, which can be easily separated from the starch macromolecular chain [9]. One approach to address this issue is through starch crosslinking, which mitigates starch retrogradation and reduces water sensitivity [18,19]. The crosslinking process requires multifunctional chemicals able to react with the hydroxyl groups of starch (and/or PVA), resulting in a biopolymer network with reduced hydrophilicity and a lower retrogradation rate [19]. Apart from some commonly used but toxic [12] starch crosslinking agents such as glutaraldehyde [20,21] and epichlorohydrin [22,23], citric acid (CA) has emerged as a biological, non–toxic and food-safe reagent for TPS crosslinking [12,18,19,24–26]. CA has three carboxylic groups per molecule which can undergo esterification reactions with hydroxyl groups in glycerol, starch, or PVA chains. This increases the hydrophobic character and the gel content, reduces migration, and then improves film properties. Early studies on crosslinked starch with CA indicated the presence of at most two esterified groups per CA at positions 1 and 5 [27]. Around 21 % of the total added CA can form diesters [26,28], while the remaining portion forms monoesters or remains unlinked, the latter potentially acting as plasticizer. However, the combined use of glycerol and CA is preferred to mitigate the excessive rigidity of TPS films [12,29]. CA esterification occurs above 50 °C, slightly earlier with glycerol than with TPS [19], while it hardly occurs with PVA [30]. In some laboratory–scale studies using the casting technique, CA is added to a pre–gelatinized starch solution at a low temperature to control and prevent crosslinking. However, in industry–oriented scalable processes using melt-mixing in an extruder, CA is added together with starch and the other additives, and gelatinization and crosslinking occur simultaneously in a reactive extrusion process where crosslinking is difficult to control [19] and negative aspects may arise.

Menzel et al. [26] prepared a TPS compound with CA and demonstrated that crosslinking may occur simultaneously with starch hydrolysis since the blending process occurs in highly acidic conditions (pH around 2), resulting in a 20 fold reduction in weight average molecular weight when using approximately 30 % of CA. Starch hydrolysis leads to an increase in the plasticizing effect, especially at high CA content, causing a significant decrease in mechanical strength [12,31]. This aspect severely limits the usefulness of CA crosslinking since, although it reduces retrogradation and hydrophilicity and increases gel content, which are positive effects, it also results in a sharp decrease in mechanical performance. Moreover, there is a substantial amount of carboxyl groups remaining in the compound, which may lead to further crosslinking in subsequent processing steps.

In this context, it has been proposed a novel approach that involves the preparation of a new type of three–dimensional plasticizer, which has a higher molecular weight than glycerol. This plasticizer is based on an esterified mixture of CA and glycerol, with an excess of glycerol to yield oligomers of esters, achieving maximum conversion of carboxyl groups. Therefore, a slower migration process due to steric hindrances could be expected. Additionally, by reaching maximum conversion of carboxyl groups, starch hydrolysis can be mitigated in a certain extent, while the crosslinking process occurs to a lesser extent during TPS compounding process and post-processing. In this work, TPS/PVA compounds with a low plasticizer migration and high gel content are expected, similar to what is achieved when using CA directly, but with improved mechanical properties as the starch hydrolysis is mitigated by the crosslinking process.

The esterification reaction between CA and glycerol has been reported in the literature for other different purposes [32]. Halpern et al. (2014) [33–36] analyzed the effect of CA/glycerol ratio, temperature and reaction time, resulting in thermosets whose degradation ability was markedly dependent on the CA conversion. Moreover, the use of CA–based esters as plasticizers has been previously reported for both conventional (PVC) [37,38] and biodegradable polymers (PLA) [39]. In these studies, bio–based triethyl citrate was used as a plasticizer, resulting in near–zero plasticizer migration. In this work, the previously reacted oligomer mixtures (OMs) were characterized and used as plasticizers in potato–based TPS/PVA compounds, maintaining a constant weight ratio of plasticizers. These compounds were compared with those containing only glycerol or a directly added CA/glycerol mixture, evaluating water solubility, migration degree, gel content and mechanical properties.

2. Experimental

2.1. Materials

Potato starch was provided by Across Organics (Geel, Belgium) and was extensively characterized in our previous works [1,15]. Its amylose content was determined by precipitation method with an amylose/amylopectin assay kit from Megazyme (Wicklow, Ireland), resulting in 20.5 % amylose. The average molecular weight obtained with gel permeation chromatography GPC–MALS (Polymer Standard Service, Mainz, Germany) and phosphorus content of the potato starch quantified by inductively coupled plasma mass spectrometer (Agilent Technologies 7700x, Waldbronn, Germany), were $6.95{\cdot}10^7$ Da and 0.043 %, respectively. The moisture content determined from the weight at 110 °C for 5 h, was 15.1 %. The particle size, surface texture and crystallinity of potato starch grains were determined by laser diffraction (Malvern Instruments, model 2000, Worcestershire, UK), scanning electron microscopy (SEM, Hitachi S3000 N, Tokyo, Japan) and X–ray diffraction (XRD, Bruker diffractometer D8–Advance model, Ettlingen, Germany). PVA 20–98 (Mw: 125000) was purchased from Sigma–Aldrich (Madrid, Spain). Glycerol and CA (99.8 % purity) were supplied by Fisher Chemical (Geel, Belgium), zinc stearate ($ZnSt_2$) by Sigma–Aldrich (Madrid, Spain) and sodium hydroxide (NaOH), by VWR Chemicals (Barcelona, Spain). All chemicals were used without further purification.

2.2. Synthesis of oligomer mixtures (OMs)

Initially, a set of mixtures containing a total of 40 g with 40 mol% CA and 60 mol% glycerol, plus 2 g of $ZnSt_2$ as catalyst [40], were thoroughly mixed in a 100 mL vial and placed in a heated and stirred vessel at 110 °C (following Halpern et al. [32]) at different times (0.15, 0.5, 1, 2, 5, 10, 24, 48 and 72 h). The conversion of CA, which acts as the limiting reactant, was determined by standardized NaOH titration (by triplicate) of the remaining carboxyl groups following the procedure previously described [41,42], with slight modifications. Beside to these mixtures, a set of six samples with different CA–glycerol molar proportions were used, all of them with a total of 40 g plus 2 g of $ZnSt_2$ and reacted in the same way as described above for 10 h, determining the CA conversion once they are cooled down to room temperature. The molar concentrations of CA were 0.5, 2.5, 5, 14, 28 and 40 mol%, always having excess of glycerol. Once reacted and converted into OMs, 24 g of each one were used as a plasticizer in further TPS/PVA compounds, were the role of $ZnSt_2$ is first as catalyst in the esterification reaction, and later as a lubricant. OMs samples with a higher initial concentration of CA resulted in more viscous mixtures, as expected, due to the lower free

glycerol content present in the mixture.

2.3. Characterization of the reaction mixtures by nuclear magnetic resonance (NMR) and infrared (IR) spectroscopy

^{1}H and ^{13}C NMR were used to identify the different species present in the OMs, in terms of structure and an extrapolation of the average molecular weight. NMR spectra were recorded on a Bruker Avance 500 MHz equipped with a 5 mm SmartProbe (BBFO ^{1}H/BB–19F). ^{1}H and ^{13}C chemical shifts δ are referenced relative to tetramethylsilane (TMS). NMR samples for molecular weight estimations using diffusion NMR were prepared by simply adding 1.0–1.3 mg of each blend together with 0.5 mL of D_2O in oven–dried 5 mm NMR tubes. PGSE NMR diffusion measurements were performed using the stimulated echo sequence and bipolar pair pulses [43]. A smoothed rectangular shape (SMSQ) was used for the gradient pulses, and their strength varied automatically during the experiments. The diffusion coefficient values (*D values*) were determined according to a method [44] described in the Supplementary information, where molecular weight distribution is calculated according to calibration with standards and applying several algorithms [45,46]. IR spectra were collected with a BRUKER IFS 66 Infrared, using an attenuated total reflectance ATR attachment.

2.4. Processing of TPS/PVA blends

TPS/PVA compounds and their corresponding films were prepared by melt-mixing following a standard procedure for TPS previously described by Domene–López et al. [9] with some modifications and subsequent thermoconformation. A total mass of 80 g containing potato starch (25%wt.), PVA (25%wt.), water (20%wt.) and OMs as plasticizer (30%wt.), were weighed and manually premixed at room temperature for 3 min. Then, the blends were processed at 110 °C in a Haake™ PolyLab™ QC Modular Torque Rheometer (ThermoFisher, Waltham, MA, USA) for 10 min; the first 5 min at 50 rpm and the last 5 min at 100 rpm. Blends obtained were subsequently processed by compression molding in a hot plates press at a pressure of 7 tons for 10 min at 160 °C, yielding 1 mm thickness sheets. Finally, the samples were cooled under pressure for 5 min. Samples were conditioned in a controlled atmosphere of relative humidity of 50 % for 48 h prior its further characterization, since the humidity affects the TPS properties [47].

A total of six different TPS/PVA blends were produced using the OMs synthesized with different CA concentration, i.e., CA0.5, CA2.5, CA5, CA14, CA28 and CA40, where the numbers denote the molar percentage of CA in the resulting OM. Two other blends of TPS/PVA were produced for comparison purposes: *i)* one blend in which only glycerol is used as plasticizer instead of OMs and therefore crosslinking is not expected. The weight fraction of glycerol is the same as the previous blends (30 %), referred to as CA0. *ii)* Another blend was prepared using a mixture of 40 mol% CA and 60 mol% glycerol as plasticizer referred to as CA40NP. This mixture was not previously reacted. All blends produced have the same total amount of plasticizer. CA0 is a standard sample using only glycerol, which is a low molecular weight plasticizer without any crosslinking properties. On the other hand, CA40NP is a standard sample that uses both glycerol and CA. CA could act on the one hand, as a crosslinker and, on the other hand, as an acid able to promote starch chains hydrolysis. In contrast, OMs exhibit a higher molecular weight, with a high level of carboxyl groups reacted. Consequently, this kind of molecules would have a lower crosslinking efficiency together lower hydrolyzing power.

2.5. Characterization of the starch/PVA blends

2.5.1. Migration degree

The migration degree of the plasticizer to the film surface was quantified using a procedure described by Marcilla et al. [48], with some modifications. Circular specimens with a diameter of approximately 7 mm and a thickness of 1 mm were prepared. These specimens were placed between two flat glasses with absorbent papers tissues on top and bottom. They were subjected to mild pressure (16.5 kPa) and kept in an oven at 60 °C for one week. The mass of the migrated plasticizer was determined by triplicate, by weighting specimens at different times (1, 2, 5 and 7 days) and calculating the weight loss with respect to the initial weight (Eq. (1)).

$$Migration\ degree\ (\%) = \left(\frac{m_0 - m_f}{m_0}\right) \times 100 \quad (1)$$

where m_o and m_f are the initial and final masses, respectively.

2.5.2. Mechanical and thermal properties

The tensile properties of the films were determined with an Instron 3344 Universal Test instrument (Norwood, MA, USA) equipped with a 2000 N load cell, following the ASTM D882–12 [49] standard. A minimum of 8 specimens per sample were tested.

Thermomechanical analysis (TMA) was carried out using a TA Instruments Q400 model (New Castle, USA). The samples were subjected to an expansion test, where they were heated from 25 to 180 °C (maximum allowed temperature) at a rate of 5 °C·min^{-1}. The heating was carried out under a nitrogen flow of 50 mL·min^{-1}, and a constant force of 0.5 N was applied. A circular and flat probe with a diameter of 3 mm was used for the analysis.

Thermogravimetric analysis (TGA) was performed using a Mettler–Toledo TGA/SDTA851e/SF/1100 model (Barcelona, Spain). Sample were heated from 25 to 700 °C at a rate of 5 °C·min^{-1}, with a nitrogen flow of 100 mL·min^{-1}.

Dynamic thermomechanical analysis (DMTA) analysis was conducted on a DMA 1 Instrument (Mettler–Toledo, Barcelona, Spain) using a dual cantilever clamp. They analysis was carried out over a temperature range of −100 °C to 60 °C, while maintaining a frequency of 1 Hz. The specimens used for this analysis had dimensions of 8.5 × 25 × 1 mm.

2.5.3. Hydration properties

The moisture content and water solubility of the films were determined using 1 × 1 cm^2 specimens following the procedures described in the literature [1,9]. Moisture content, expressed as percentage (grams in 100 g of sample), was calculated as shown in Eq. (2), by the difference between the initial mass of the sample (m_o) and the mass after drying at 110 °C for 5 h (m_1). Measurements were taken in quintuplicate.

$$Moisture\ content(\%) = \left(\frac{m_0 - m_1}{m_0}\right) \times 100 \quad (2)$$

After that, the water solubility of each sample was measured by placing the dried films individually in 10 mL tubes filled with 9 mL of distilled water. The tubes were capped and stored at 25 °C for 24 h. Subsequently, they were taken out and dried again at 110 °C for 5 h to determinate the final dried mass (m_f). Therefore, the solubility in water was calculated from the weight loss of soluble matter as follows (Eq. (3)).

$$Solubility\ in\ water\ (\%) = \left(\frac{m_0 - m_f}{m_0}\right) \times 100 \quad (3)$$

The results were obtained in quintuplicate.

The gel content in water was determined by placing specimens (with dimensions of 2 × 2 cm^2), previously dried at 110 °C for 5 h, in 250 mL of distilled water at 80 °C for 24 h under stirring. The gel content (Eq. (4)) was calculated from the difference between the weight of the dried starting sample (m_1) and the dried weight of the remaining specimen that did not pass through a stainless–steel mesh with an aperture of 50 μm, used as a filter, after 5 h at 100 °C (m_f).

$$Gel\ content\ (\%) = \left(\frac{m_f}{m_1}\right) \times 100 \quad (4)$$

Furthermore, the swelling degree (Eq. (5)) was determined from weight of the dried starting sample (m_1) and weight of the undissolved samples (when possible), after removing surface water using a tissue paper (m_2), and before its last dried for 5 h in an oven used to determine the gel content [18]. Measurements were taken in quintuplicate.

$$Swelling\ degree\ (\%) = \left(\frac{m_2 - m_1}{m_1}\right) \times 100 \quad (5)$$

3. Results and discussion

3.1. Characterization of OMs

Fig. S1 shows the evolution of the conversion degree of OMs over time, using an initial CA concentration of 40 mol%. Glycerol is in excess due to, on the one hand, each CA molecule has three carboxyl groups that can react with an equivalent number of hydroxyls in glycerol and, on the other hand, the literature reveals that each CA molecule might form up to two esters [27]. After 72 h, the maximum conversion achieved is 61.4 % (1.80 ester groups per CA molecule). However, at 10 h, a conversion of 55 % (1.65 ester groups per CA molecule) has already been reached. This result indicates that most of the esterification occurs within the first 10 h. This observation is further supported by the peak at 1180 cm^{-1} in the ATR–FTIR spectra of samples reacted at different times, as shown in Fig. S2.

On the other hand, the ^{1}H NMR spectrum reveals that OMs starting with 40 mol% of CA for 10 h of reaction exhibit an average of 1.7 glyceryl units per citric moiety unit. It is worth noting that the reaction conditions are similar to those employed in the subsequent process used for blend production. Therefore, it is not expected that a significant number of additional ester groups are formed during the subsequent TPS/PVA compounding.

Although there is limited information in the literature regarding the structural NMR characterization of poly(glycerol citrate) itself, some reports provide insight into the acid ester ratio based on ^{13}C NMR data [50,51], or the ratio of glycerol units to citrate units in the final hyperbranched oligomer based on ^{1}H NMR spectral integrals [52]. In this study, ^{1}H NMR spectrum confirms that OMs starting with 40 mol% of CA and 10 h of reaction exhibit an average of 1.7 glyceryl units per citric moiety unit. The detailed justification for this finding is described in the Supplementary information. This confirms the result obtained from the conversion of 1.65 esters per CA. Therefore, once again, it is not expected that a significant number of additional ester groups are formed during the subsequent TPS/PVA compounding.

Molecular weight analysis of the OM with 40 mol% CA was also conducted using NMR spectroscopy, as described in previous studies [45,46,53]. Table 1 shows the estimated values of D, hydrodynamic radii and average molecular weight obtained from diffusion NMR measurements. Fig. 1 shows the weight–average molecular weight on different fractions. Approximately, 7%wt. of the OM corresponds to non–reacted glycerol, while all other fractions contain bonded moieties. Interestingly, more than 65 % of the oligomers exhibit higher molecular weights within the range of 764–2060 Da, with the most prevalent population being 1081 Da representing a 30 % of the overall species. This population roughly corresponds to four CA molecules diesterified alternatively with glycerol.

Table 1
Diffusion coefficients (D), hydrodynamic radius (r_H) and weight–average molecular weight (M_w), at 295 K in D_2O.

D (10^{-9} $m^2 \cdot s^{-1}$)[a]	r_H (A)	M_w (Da)[b]	Fraction (%)
0.2203	9.8 ± 0.5	2060 ± 194	13.6
0.3170	6.8 ± 0.3	1086 ± 72	29.8
0.3871	5.6 ± 0.2	764 ± 44	22.4
0.5324	4.1 ± 0.2	436 ± 38	10.0
0.6082	3.5 ± 0.1	345 ± 15	10.0
0.7371	2.9 ± 0.2	249 ± 22	7.2
1.0828	2.0 ± 0.1	125 ± 8	7.0

[a] The experimental error in the D values is ±2 %.
[b] Determined by ^{1}H PGSE diffusion NMR according to procedure described and discussed in Supplemental information.

3.2. Film characterization

The visual appearance of the films obtained by hot pressing of melt–mixed TPS/PVA compounds is shown in Fig. 2. The texture of the films is transparent when only glycerol is used as plasticizer, and it becomes yellowish when using CA in OM, the higher the CA concentration, the higher the yellowish intensity. In addition, the highest yellowish intensity is observed for CA40NP sample, where the CA was directly added to the formulation, which is in good agreement with other researchers [20,29,54,55]. These yellowish intensities were confirmed and metrically measured by applying CIELab color space analysis to the specimens shown in Fig. 2, shown in Table S3 of the Supplementary information. It is stated, for all the specimens, middle values in lightness parameter (L) and white neutral ones for a* were obtained; rather, there is a clear increase for b* from slightly white shade into more intense yellow shade as far as CA increases its concentration in OMs, with the highest value when CA is directly added to the compound. This could be attributed to the potential formation of dextrins resulting from starch hydrolysis by the action of CA [25,56]. Interestingly, the color in the CA40NP sample is much more intense than in CA40 film, indicating a reduced extent of starch hydrolysis when the OM with an equivalent CA–glycerol ratio is used.

Fig. 3 shows the evolution of the migration degree in TPS/PVA blends over time for all the blends tested. The migration rate is higher in the first 24 h of testing, and thereafter, the degree remains relatively constant, approaching a plateau. As it can be observed, there is a clear correlation with the initial CA content in the OM. In the first place, the films without OM (i.e., CA0 and CA40NP), show higher migration degrees, resulting in weight losses of 10.6 and 9.7 %, respectively. In contrast, all the films processed with OM show lower migration, with the migration degree decreasing as the initial CA concentration in the OM increases. Thus, it can be noticed a reduction in migration of 6.98 % for CA40 film, corresponding to a relative reduction of 70 % compared to the CA0 sample. These results can be attributed to the increase in the molecular weight of the new plasticizer [9,39], as well as the steric hindrance caused by the three–dimensional structure of some of the oligomers. The CA0 sample showed higher migration due to two main factors: firstly, glycerol (used as plasticizer) has a lower molecular weight compared to the other OMs produced; and secondly, the CA0 sample contains a higher amount of glycerol than the others. The film plasticized with glycerol and CA (CA40NP) shows a high migration degree as well, which can be explained by prominent starch hydrolysis that leads to a significant reduction in starch molecular weight. Additionally, the excess of CA acts as an internal and external plasticizer [57,58], facilitating its migration to the surface of the biomaterial. Since migration occurs through the retrogradation of starch, this phenomenon is more likely to happen when the starch chains are shorter and more flexible, which precisely occurs after the hydrolysis [59].

Therefore, it is concluded that the problem of plasticizer migration to the surface of the TPS/PVA films can be reduced in an effective way by using these three–dimensional OMs as plasticizer.

The tensile properties of all TPS/PVA compounds studied are shown in Fig. 4. It can be observed that samples with low CA content in the OM, i.e., CA0.5, CA2.5 and CA5 samples, exhibit a slight decrease in Young's modulus, constant tensile strength, and a mild increase in elongation at break compared to the reference film plasticized with glycerol (CA0). Jiugao et al. [60] reported a plasticizing effect of CA at relatively lower CA contents (up to 3 %), which was attributed to the strong interactions

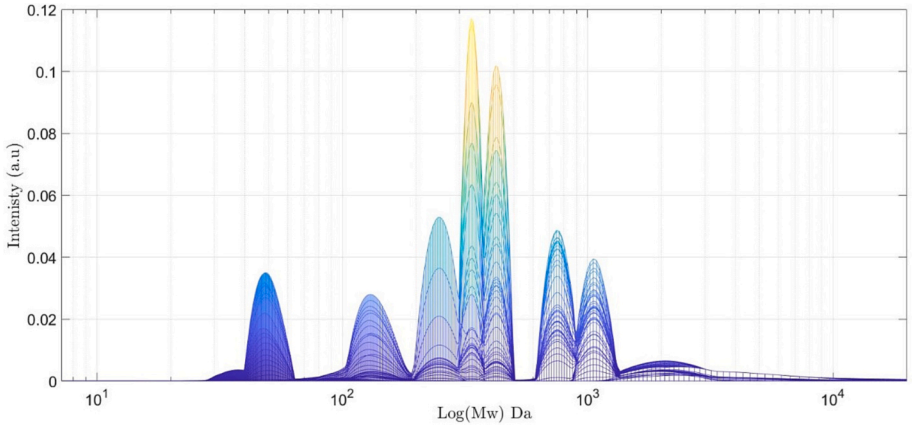

Fig. 1. Molecular weight distribution of the OM of 40 mol% CA and 60 mol% glycerol reacted after 10 h at 110 °C.

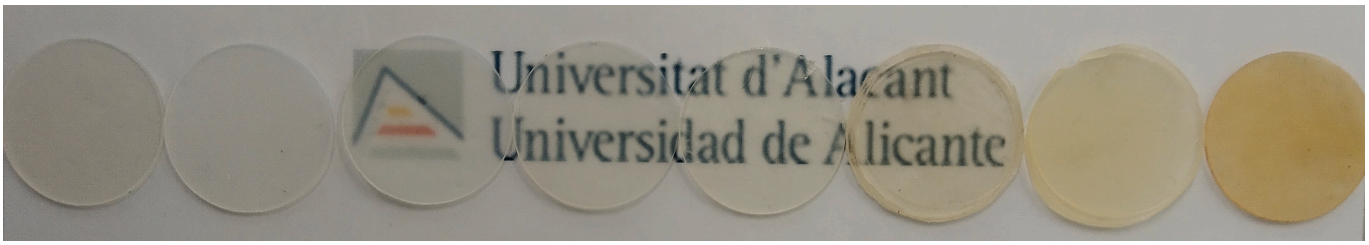

Fig. 2. Visual appearance of the sheets obtained. From left to right: CA0, CA0.5, CA2.5, CA5, CA14, CA28, CA40 and CA40NP.

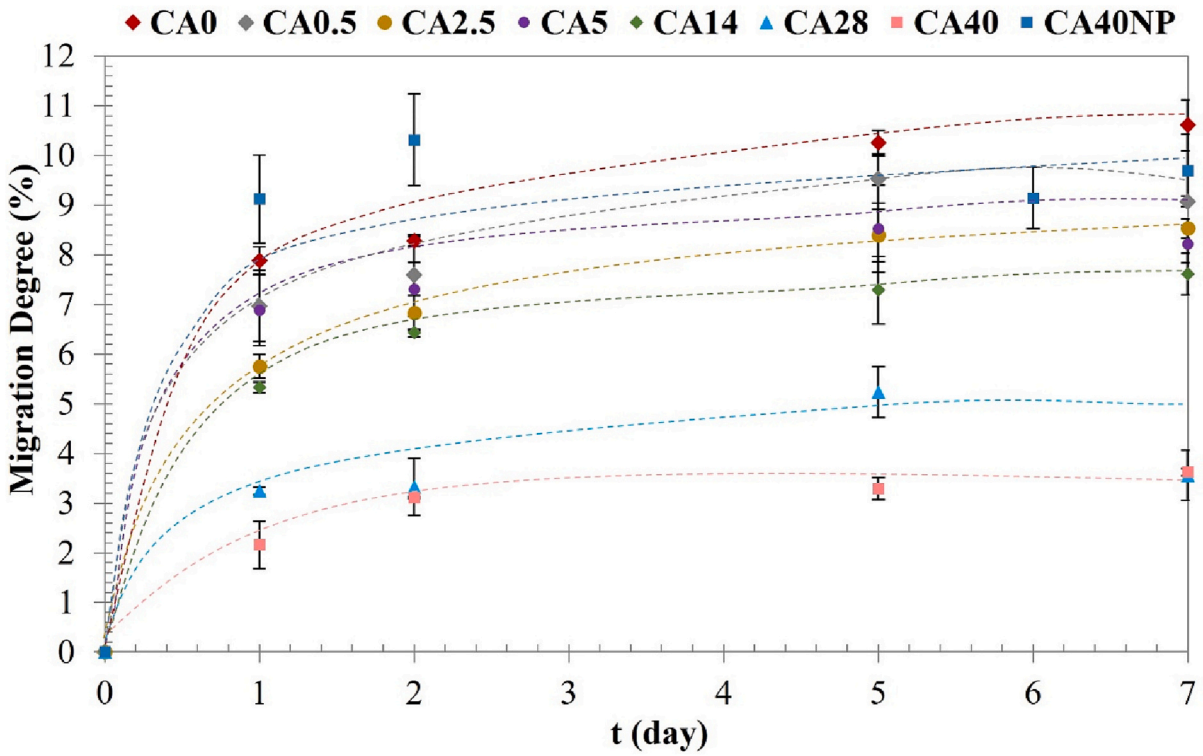

Fig. 3. Migration degree as a function of time and CA content of TPS/PVA blends using the OM as plasticizer.

between the acid and starch, disrupting the interactions between starch molecules. However, the acid concentrations employed in the present work are relatively higher, and based on the results, the observed behavior in Fig. 4A for CA5 and below can be also attributed to starch hydrolysis promoted by the acid. Nevertheless, a different trend is observed with higher CA content in the OM. The Young's modulus shows a sharp increase from 10 MPa for the blend plasticized with only glycerol to 26 MPa for CA28 and 21 MPa for CA40.Interestingly, higher tensile strength and elongation at break for both samples compared to CA0 were exhibited, indicating significantly improved toughness.

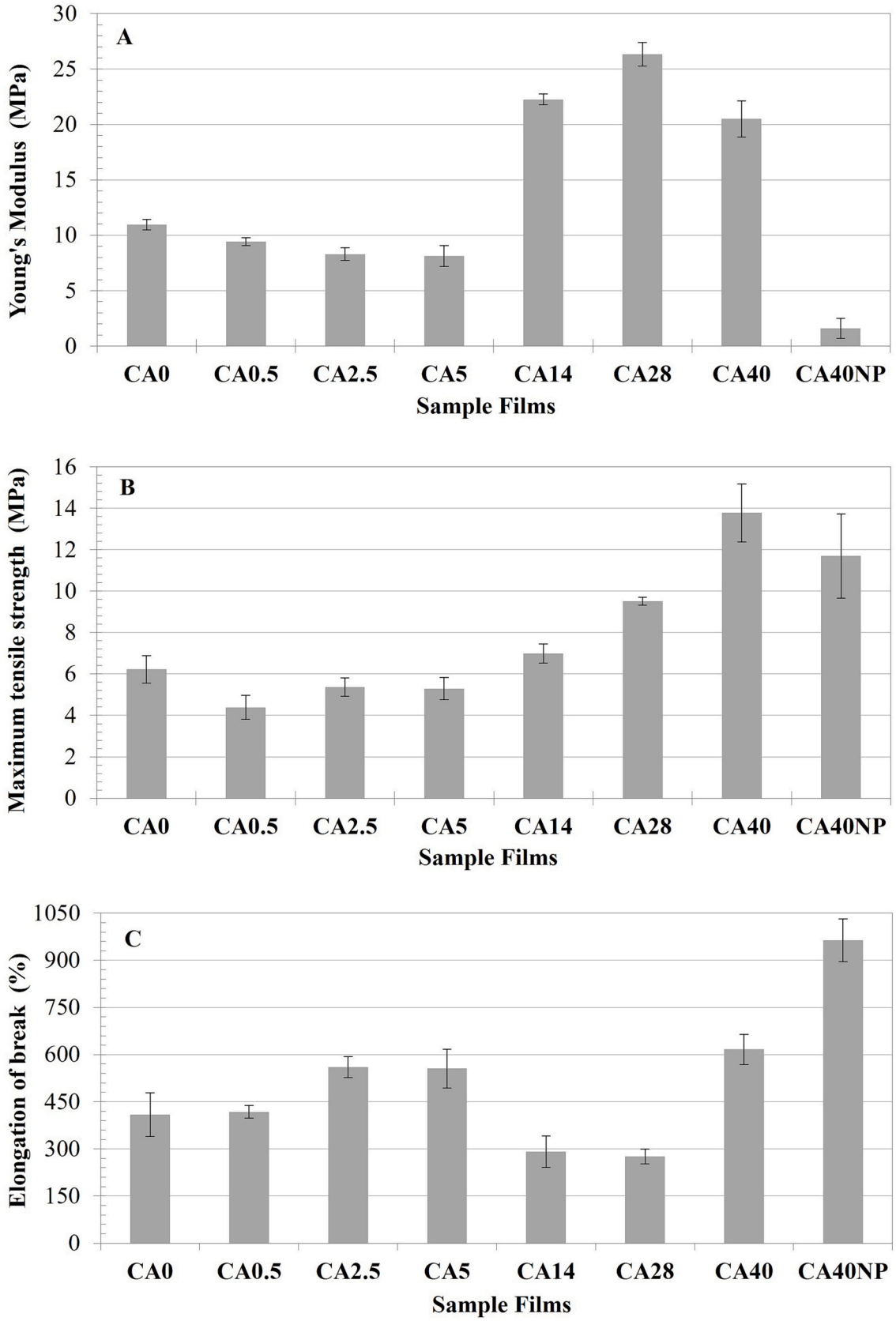

Fig. 4. Tensile properties of starch/PVA blends. A) Young's modulus (MPa); B) maximum tensile strength (MPa); C) elongation at break (%).

Similar trends were reported by Zdanowicz et al. [61] who used choline citrate (instead of CA) and glycerol to prepare starch films. It is worth noting that the CA40NP sample, sample plasticized with both CA and glycerol, exhibits the lowest Young's modulus and the highest elongation at break. The stiffest sample is the CA28 sample, which is attributed to the use of a high molecular weight plasticizer with a three–dimensional structure and some crosslinking ability. The CA40 sample shows a slight decrease in modulus but an increase in both tensile strength and elongation. This can be due to the presence of more available free carboxyl groups in the CA40 sample, which hydrolyze the starch, resulting in a slight decrease in performance compared to the CA28 sample (Fig. S9). On the contrary, when CA is directly added to the formulation, as the case of CA40NP, the presence of free carboxyl groups promotes extensive starch hydrolysis, leading to the transformation of starch into smaller molecules. This makes the higher crosslinking irrelevant, as indicated by the lowest modulus and the observed yellowish color in Fig. 2. Therefore, it seems that a high content of free carboxyl groups leads to a major hydrolysis of the starch and the resulting molecules act as plasticizer, modifying the mechanical properties, i.e., diminishing the Young's modulus and increasing the elongation at break. Comparing the mechanical properties found in this work with results reported by other authors such as Trinath et al. [62] who have also worked with TPS/PVA compounds, it is possible to state that samples obtained in the present work show a remarkable much higher values of elongation at break (up to 600 %).

Thermomechanical analysis (TMA) is a technique used to measure the dimensional deformation in films [63] providing information about potential changes in the softening point of samples [64]. The relationship between the thickness of the sheets during heating and its initial value (l/l_0) as a function of temperature is shown in Fig. 5. The CA0 and CA5 samples exhibit the typical behavior of samples with a progressive softening process which occurs around 160 °C. In the case of CA5, the softening point is shifted to lower temperatures, probably due to the plasticizing effect of the acidic pH, leading to starch hydrolysis caused by the small amount of the OM. However, the OMs with higher CA ratios, i.e., CA28 and CA40, and sample plasticized with both glycerol and CA, i.e., CA40NP, show a significant reduction in probe penetration at high temperatures. Their TMA curves display less dependence on temperature, exhibiting the typical behavior of a thermoset. The CA28 formulation seems to be less crosslinked than CA40 and CA40NP. These results suggest that crosslinking occurs at acid concentrations above CA28. The OM used in the CA28 formulation seems to produce fewer intercatenary insertions with the starch chains compared to the OM synthetized with 40 mol% CA, where acid hydrolysis yields smaller insertion spaces. This effect is more pronounced when CA is directly added to the formulation (CA40NP).

Furthermore, a small volume change can be observed in the curve of the CA0 sample around 170 °C. If the TMA pattern is correlated with the DTGA curve (inset picture of Fig. 5), it is possible to confirm that this change in the CA0 sample corresponds to the loss of intrinsic moisture and the loss of glycerol, which is more prone to migration. When comparing the changes in all curves, this behavior is only observed in the case of CA0, which uses glycerol as the sole plasticizer.

Fig. 6 shows the variations of the loss tangent (tan δ) and the storage modulus (G′) in the temperature sweep ranging from −100 to 60 °C at a constant frequency (1 Hz). The tan δ behavior of the films is presented in Fig. 6A. For samples with low CA content in the reaction (CA0, CA0.5, CA2.5 and CA5), tan δ exhibits two maxima corresponding to two different relaxations very probably attributed to the fact that at certain glycerol concentrations, percolated paths of glycerol can be formed, obtaining a less well–dispersed system and potential phase separation which could eventually be reflected in two different glass transitions/relaxations.

The first peak, known as the β–relaxation, placed at −68 °C and could be attributed to a glycerol–starch–rich phase. The second peak, the α–relaxation, placed at a temperature between −30 and −10 °C and corresponds to starch/PVA [9]. According to Zdanowicz et al. [61] the β–relaxation is assigned to a movement of small molecules of plasticizers and moisture. The higher content of CA the higher temperature of the β–peak and the lower intensity related to movement restriction caused by e.g., crosslinking, or higher compatibility. In addition, according to the literature, when the glycerol concentration is below 25 % no

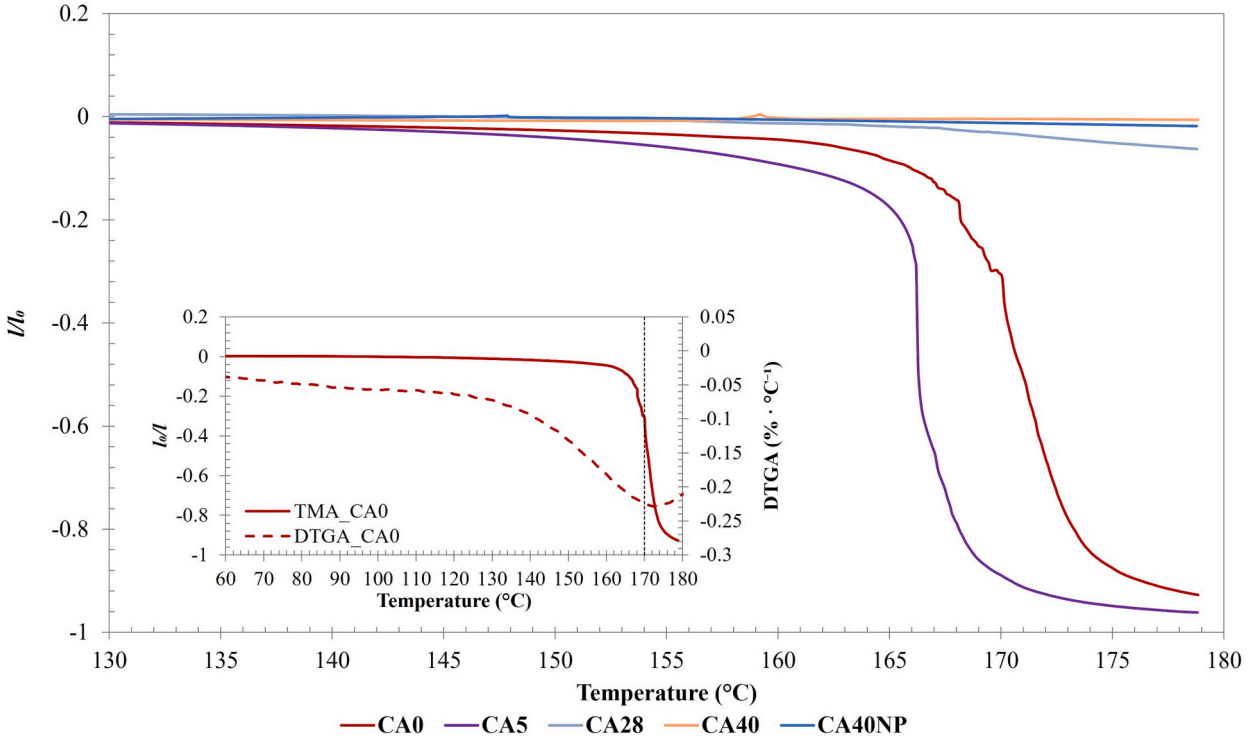

Fig. 5. TMA of TPS/PVA blends.

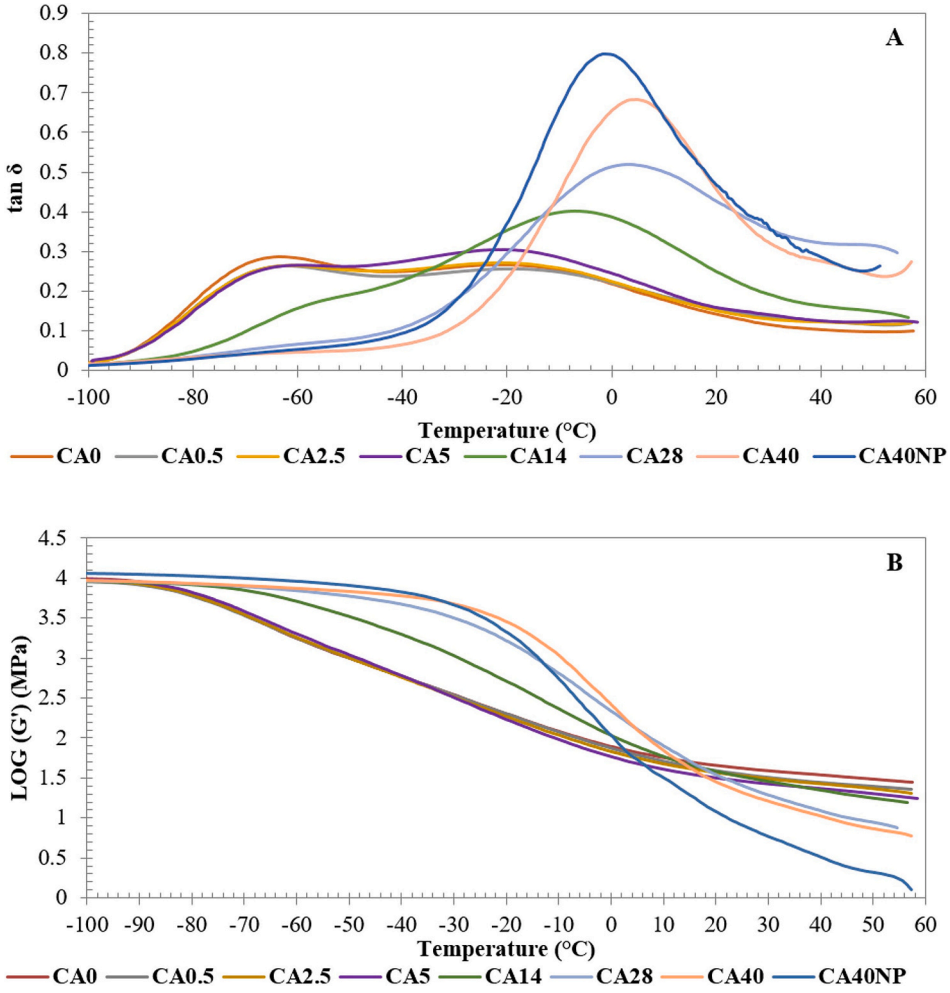

Fig. 6. Evolution of A) loss tangent (tan δ) and B) storage modulus with temperature for all TPS/PVA samples studied at a constant frequency of 1 Hz.

anisotropy and good dispersion is observed [65], and hence the absence of glass transition at low temperatures in DMTA (Fig. 6) could explain in terms of relative low concentrations of unreacted glycerol. For instance, at CA ratios above 14 mol% in the synthetized OM, the availability of glycerol decreases, suggesting that glycerol may not be in clear excess. As a result, the −68 °C peak diminished at CA14, and disappears for higher CA contents. These results could indicate that, as expected, in the case of the CA40 sample, glycerol has extensively reacted during OM synthesis. In the case of CA40NP, crosslinking and reaction between carboxylic CA groups and starch hydroxyl groups have occurred, as reflected in the TMA results (Fig. 5).

The second peak in tan δ shows a progressive shift to higher temperatures as the CA concentration in the OM is increased. This aspect suggests that starch interacts with a plasticizer of higher molecular weight in addition to the possibility of some crosslinking. It is worth mentioning that in the case of CA40NP the transition occurs at a temperature slightly lower than in the case of CA40. This could be due to the fact that CA40 uses OM of relatively high molecular weight, sample where starch has not been hydrolyzed in the same extent than in the case of CA40NP which higher ratio of free acid groups seems to have promoted starch hydrolysis. This is clearly evidenced by the sharp decrease in storage modulus observed in CA40NP compared to the other samples (Fig. 6B). This is also reflected in tensile modulus results shown in Fig. 4A.

Table 2 shows the results obtained for the hydration properties. Water content and solubility in water are important properties since they can be limiting factors of the material to determine its final application.

Table 2
Moisture content, solubility, gel content and swelling degree corresponding to all TPS/PVA compounds studied.

Sample	Moisture content (%)	Solubility in water (%)	Gel content (%)	Swelling degree (%)
CA0	14.6 ± 0.2	41.9 ± 0.8	7.16 ± 2.01	NA
CA0.5	18.6 ± 0.5	42.0 ± 0.2	0.910 ± 4.839	NA
CA2.5	16.8 ± 0.4	49.2 ± 0.6	1.02 ± 5.26	NA
CA5	15.0 ± 0.4	56.0 ± 0.5	0.563 ± 0.437	NA
CA14	9.72 ± 0.15	55.1 ± 0.7	0.784 ± 6.699	NA
CA28	7.33 ± 0.41	49.6 ± 1.4	38.5 ± 3.5	431 ± 54
CA40	7.15 ± 0.31	47.0 ± 0.5	47.3 ± 1.9	217 ± 23
CA40NP	7.90 ± 0.14	43.8 ± 0.4	51.1 ± 0.9	129 ± 3

NA (not available): the sample was disintegrated, and its swelling behavior could not be determined.

As CA content is increased in the OM, the likely hydrolysis, visually shown by the yellowish color in Fig. 2, could promote a slight or almost negligible increase of the moisture content in CA0.5, CA2.5 and CA5 samples (14–18 %). As crosslinking increases due to the presence of more available carboxyl groups, the formation of a network structure leads to an increase in gel content and a decrease in moisture content. This is attributed to the increased difficulty of water to diffuse within the network. Thus, water content significantly decreased for higher CA

concentrations reaching a value of 7.15 % when using 40 mol% of acid.

Concerning solubility in water, the inclusion of OMs in the formulation leads to an increase of this parameter. Similar results were found by Zdanowicz et al. [61] using a system of TPS plasticizers based on choline citrate and glycerol. This increase in solubility is probably due to the presence of unreacted carboxyl groups, which contributes to the polar stability of the samples and consequently enhance their solubility. Among the samples studied, CA5 and CA14 exhibit the highest solubility values, with 56.0 % and 55.1 %, respectively.

As the crosslinking becomes more pronounced in the formulation, the polar character of the samples decreases, resulting in a moderate reduction in solubility for CA28 (49.6 %) and CA40 (47.0 %). Additionally, in the case of CA40NP, which exhibits both a high starch hydrolysis rate and a significant crosslinking degree, the polar character decreases further, leading to a slightly lower solubility of 43.8 %.

It is worth noting that the solubility of biopolymer–based films is closely related to their biodegradability [66]. Therefore, the inclusion of OMs in the formulation promotes faster degradation under water immersion.

Table 2 also shows the gel content and swelling degree of the samples. It is important to note that the determination of swelling degree was possible only for those specimens that maintained their integrity. Both properties are closely related since the gel content is related to the mass of biopolymer involved in the formation of a crosslinked network, while the crosslinking density of this network influences the swelling degree [22].

It was observed that the formulation without CA cannot be fully dissolved in water, showing a gel content of approximately 7.2 %. When CA is included in the formulation (CA5), the gel content decreases, likely due to starch hydrolysis, in good agreement with the yellowish appearance of the samples in Fig. 2. Gel content is almost cero in a wide range, but when CA content reaches a value (CA28), crosslinking could overcome hydrolysis provoking a marked increase in gel content up to 38.5 % (CA28) and 47.3 % (CA40). This suggests that the presence of free CA and free acid species in the oligomer promotes crosslinking to some extent, as expected. When a mixture of glycerol and CA is directly included in the formulation (CA40NP) a slightly higher gel content is observed, indicating the presence of a highly crosslinked compact network with highly hydrolyzed and degraded starch. This observation is consistent with the swelling values, which are lower for CA40NP than CA40.

The swelling value of CA28 is twice that of CA40, result that has a great relevance from the point of view that high molecular weight crosslinkers result in less compact structures, allowing for greater swelling. CA28 presents high swelling, low moisture content, and appreciable gel content, indicating crosslinking (as also shown by TMA in Fig. 5). The presence of a crosslinked structure with low–density interconnections (resulting from the high molecular weight crosslinker with limited hydrolyzed starch) creates voids among branches to accommodate more solvent. Consequently, the degradation rate under water is higher; at the same time, CA28 formulation was also the stiffest one.

These results can be interpreted according to Fig. 7, which compares the crosslinking density achieved using a low molecular weight and aggressive crosslinker, resulting in high crosslinking but low swelling, low stiffness in part promoted by starch hydrolysis. Additionally, the results have allowed noticing that high molecular weight plasticizers with some crosslinker effect, provide certain stiffness, integrity and swelling, while maintaining low moisture content.

On the contrary, the swelling of CA28 and CA40 samples decreased as the content of OM increases, indicating that these films also have a more compact network by the own structure of the new plasticizer. The OM has a three–dimensional structure, and its average molecular weight is higher than raw CA or glycerol.

4. Conclusion

The following conclusions have been stated in the present work:

- The preparation of OMs based on polyesterified citrates, in a separate and previous step from glycerol and CA, resulted in valid plasticizers for TPS/PVA compounds, with highly improved properties compared to directly using CA and glycerol in the TPS gelatinization, blending and compounding.

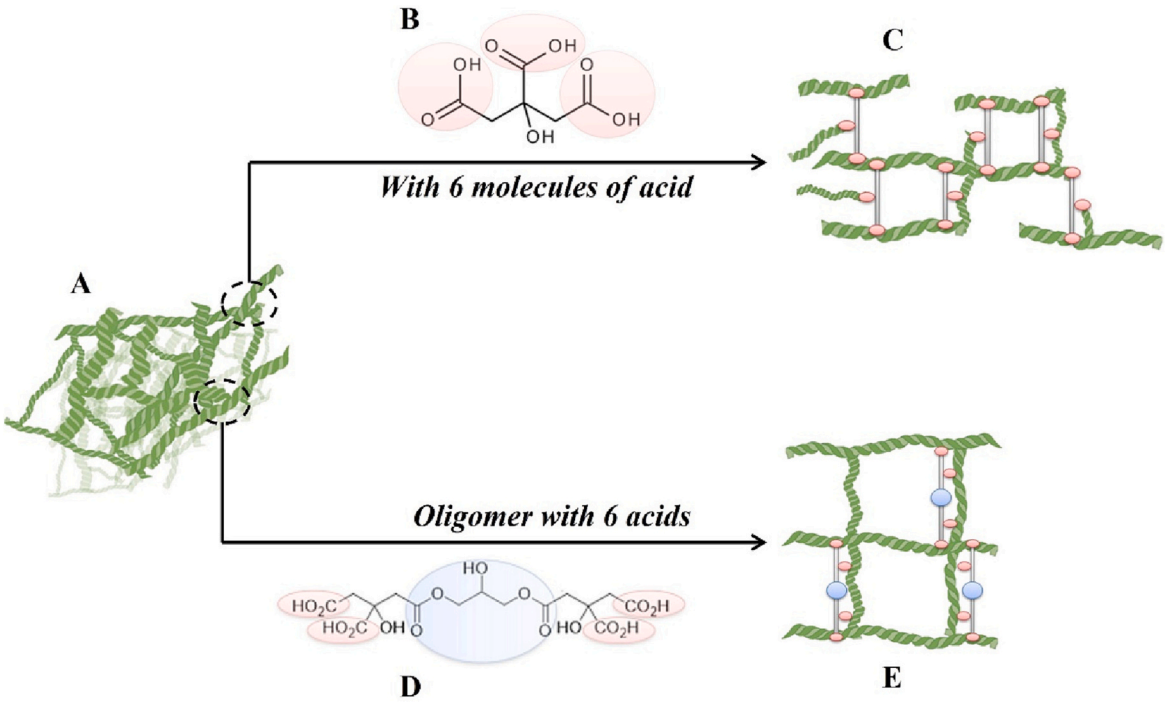

Fig. 7. Scheme of the structure of TPS plasticized with OM and TPS with CA: A) structure of thermoplastic starch (TPS); B) chemical formula of CA; C) TPS with 6 molecules of CA on its structure; D) chemical formula of a 1,3-linear glyceridic unit (1,3L); E) TPS plasticized with OM of 6 acids.

- The OMs, which are synthetized in excess of glycerol and have a three-dimensional structure, present a composition where 65 % of them have molecular weights between 764 and 2060 Da. Regardless molar excess of glycerol, the maximum yield with respect carboxyl groups was around 60 %, a close value to the maximum reported of two esters per CA molecule.
- TPS/PVA compounds prepared using these OMs as plasticizers, of high molecular weight, some crosslinking activity, and low acidic–polar character, present many advantages with respect using raw crosslinkers: it performs higher stiffness, lower migration degree, lower moisture, higher swelling and maintained degradability upon water immersion.

Nevertheless, further studies are required to improve some of the features of the materials designed in this study in order to expand their applications. On the one hand, an increase of the maximum tensile strength can be interesting to obtain materials that can be used as high resistance bioplastic packaging. On the other hand, a moderate increase of the gel content could lead to more durable materials for long-term packaging applications. As conclusion, a new generation of plasticizers can be developed, with higher molecular weight, which considerably reduces the plasticizer migration and provide mechanical consistence and stability to TPS based compounds.

CRediT authorship contribution statement

J.M.C: methodology, procedures, formal analysis, writing – original draft; M.G.M: conceptualization, formal analysis, supervision, writing; N.M.P: methodology, procedures, formal analysis of the NMR; D.D.L: conceptualization, formal analysis, supervision, writing; J.M.P: methodology, procedures, formal analysis of the NMR, writing; F.M.A.C: methodology, procedures, formal analysis of the NMR, writing; I.F: methodology, procedures, formal analysis of the NMR, writing; I.M.G: project administration, funding acquisition, supervision; J.C.G.Q: supervision, formal analysis, writing, project administration.

Declaration of competing interest

The authors declare that they have no known competing financial interests or personal relationships that could have appeared to influence the work reported in this paper.

Acknowledgements

This work was partially supported by the Spanish Ministry of Science and Ministry of Economy, Industry and Competitiveness and the Spanish MINECO (PID2019-108632RB-l00 and PID2021-126445OB-I00, respectively) and Generalitat Valenciana (PROMETEO CIPROM/2021/027). This work was also partially supported by the TED2021-130389B-C21 research project, funded by MCIN/AEI/10.13039/501100011033 and by the European Union NextGenerationEU/PRTR. Juana M. Pérez acknowledges support from University of Almería (HIPATIA2021_04 fellowship).

Appendix A. Supplementary data

Supplementary data to this article can be found online at https://doi.org/10.1016/j.ijbiomac.2023.125478.

References

[1] D. Domene-López, J.C. García-Quesada, I. Martin-Gullon, M.G. Montalbán, Influence of starch composition and molecular weight on physicochemical properties of biodegradable films, Polymers 11 (2019) 1–17, https://doi.org/10.3390/polym11071084.
[2] J.M. Castro, M.G. Montalbán, D. Domene-López, I. Martín-Gullón, J.C. García-Quesada, Study of the plasticization effect of 1-ethyl-3-methylimidazolium acetate in TPS/PVA biodegradable blends produced by melt-mixing, Polymers 15 (2023) 1788, https://doi.org/10.3390/polym15071788.
[3] G. Sanchez-Olivares, S. Rabe, R. Pérez-Chávez, F. Calderas, B. Schartel, Industrial-waste agave fibres in flame-retarded thermoplastic starch biocomposites, Compos. Part B 177 (2019), 107370, https://doi.org/10.1016/j.compositesb.2019.107370.
[4] Y. Qin, Y. Liu, X. Zhang, J. Liu, Development of active and intelligent packaging by incorporating betalains from red pitaya (Hylocereus polyrhizus) peel into starch/polyvinyl alcohol films, Food Hydrocoll. 100 (2020), 105410, https://doi.org/10.1016/j.foodhyd.2019.105410.
[5] H. Tian, J. Yan, A.V. Rajulu, A. Xiang, X. Luo, Fabrication and properties of polyvinyl alcohol/starch blend films: effect of composition and humidity, Int. J. Biol. Macromol. 96 (2017) 518–523, https://doi.org/10.1016/j.ijbiomac.2016.12.067.
[6] C.A. Gómez-Aldapa, G. Velazquez, M.C. Gutierrez, E. Rangel-Vargas, J. Castro-Rosas, R.Y. Aguirre-Loredo, Effect of polyvinyl alcohol on the physicochemical properties of biodegradable starch films, Mater. Chem. Phys. 239 (2020), 122027, https://doi.org/10.1016/j.matchemphys.2019.122027.
[7] A.A. Aydin, V. Ilberg, Effect of different polyol-based plasticizers on thermal properties of polyvinyl alcohol:starch blends, Carbohydr. Polym. 136 (2016) 441–448, https://doi.org/10.1016/j.carbpol.2015.08.093.
[8] Y. Liu, X. Mo, J. Pang, F. Yang, Effects of silica on the morphology, structure, and properties of thermoplastic cassava starch/poly(vinyl alcohol) blends, J. Appl. Polym. Sci. 133 (2016) 1–9, https://doi.org/10.1002/app.44020.
[9] D. Domene-López, M.M. Guillén, I. Martin-Gullon, J.C. García-Quesada, M. G. Montalbán, Study of the behavior of biodegradable starch/polyvinyl alcohol/rosin blends, Carbohydr. Polym. 202 (2018) 299–305, https://doi.org/10.1016/j.carbpol.2018.08.137.
[10] R. Abedi-Firoozjah, N. Chabook, O. Rostami, M. Heydari, A. Kolahdouz-Nasiri, F. Javanmardi, K. Abdolmaleki, A.M. Khaneghah, PVA/starch films: an updated review of their preparation, characterization, and diverse applications in the food industry, Polym. Test. 118 (2023), 107903, https://doi.org/10.1016/j.polymertesting.2022.107903.
[11] M. Zamanian, H. Sadrnia, M. Khojastehpour, F. Hosseini, B. Kruczek, J. Thibault, Barrier properties of PVA/TiO2/MMT mixed-matrix membranes for food packaging, J. Polym. Environ. 29 (2021) 1396–1411, https://doi.org/10.1007/s10924-020-01965-8.
[12] A. Das, R. Uppaluri, C. Das, Feasibility of poly-vinyl alcohol/starch/glycerol/citric acid composite films for wound dressing applications, Int. J. Biol. Macromol. 131 (2019) 998–1007, https://doi.org/10.1016/j.ijbiomac.2019.03.160.
[13] M. Belén, K. Encalada, E. Proaño, An overview of starch-based biopolymers and their biodegradability, Cienc. Ing. 39 (2018) 245–258.
[14] K. Junlapong, P. Boonsuk, C. Chaibundit, S. Chantarak, Highly water resistant cassava starch/poly(vinyl alcohol) films, Int. J. Biol. Macromol. 137 (2019) 521–527, https://doi.org/10.1016/j.ijbiomac.2019.06.223.
[15] D. Domene-López, J.J. Delgado-Marín, I. Martin-Gullon, J.C. García-Quesada, M. G. Montalbán, Comparative study on properties of starch films obtained from potato, corn and wheat using 1-ethyl-3-methylimidazolium acetate as plasticizer, Int. J. Biol. Macromol. 135 (2019) 845–854, https://doi.org/10.1016/j.ijbiomac.2019.06.004.
[16] C.L. Luchese, P. Benelli, J.C. Spada, I.C. Tessaro, Impact of the starch source on the physicochemical properties and biodegradability of different starch-based films, J. Appl. Polym. Sci. 135 (2018) 46564, https://doi.org/10.1002/app.46564.
[17] O. Lopez, M.A. Garcia, M.A. Villar, A. Gentili, M.S. Rodriguez, L. Albertengo, Thermo-compression of biodegradable thermoplastic corn starch films containing chitin and chitosan, LWT Food Sci. Technol. 57 (2014) 106–115, https://doi.org/10.1016/j.lwt.2014.01.024.
[18] H. Wu, Y. Lei, J. Lu, R. Zhu, D. Xiao, C. Jiao, R. Xia, Z. Zhang, G. Shen, Y. Liu, S. Li, M. Li, Effect of citric acid induced crosslinking on the structure and properties of potato starch/chitosan composite films, Food Hydrocoll. 97 (2019), 105208, https://doi.org/10.1016/j.foodhyd.2019.105208.
[19] P.G. Seligra, C. Medina Jaramillo, L. Famá, S. Goyanes, Biodegradable and non-retrogradable eco-films based on starch-glycerol with citric acid as crosslinking agent, Carbohydr. Polym. 138 (2016) 66–74, https://doi.org/10.1016/j.carbpol.2015.11.041.
[20] H. Li, X. Gao, Y. Wang, X. Zhang, Z. Tong, Comparison of chitosan/starch composite film properties before and after cross-linking, Int. J. Biol. Macromol. 52 (2013) 275–279, https://doi.org/10.1016/j.ijbiomac.2012.10.016.
[21] B. Ramaraj, Crosslinked poly(vinyl alcohol) and starch composite films. II. Physicomechanical, thermal properties and swelling studies, J. Appl. Polym. Sci. 103 (2007) 909–916, https://doi.org/10.1002/app.25237.
[22] K. Das, D. Ray, N.R. Bandyopadhyay, A. Gupta, S. Sengupta, S. Sahoo, A. Mohanty, M. Misra, Preparation and characterization of cross-linked starch/poly(vinyl alcohol) green films with low moisture absorption, Ind. Eng. Chem. Res. 49 (2010) 2176–2185, https://doi.org/10.1021/ie901092n.
[23] B. Sreedhar, D.K. Chattopadhyay, M.S.H. Karunakar, A.R.K. Sastry, Thermal and surface characterization of plasticized starch polyvinyl alcohol blends crosslinked with epichlorohydrin, J. Appl. Polym. Sci. 101 (2006) 25–34, https://doi.org/10.1002/app.23145.
[24] J. Jose, M.A. Al-Harthi, Citric acid crosslinking of poly(vinyl alcohol)/starch/graphene nanocomposites for superior properties, Iran. Polym. J. 26 (2017) 579–587, https://doi.org/10.1007/s13726-017-0542-0.
[25] N. Reddy, Y. Yang, Citric acid cross-linking of starch films, Food Chem. 118 (2010) 702–711, https://doi.org/10.1016/j.foodchem.2009.05.050.
[26] C. Menzel, E. Olsson, T.S. Plivelic, R. Andersson, C. Johansson, R. Kuktaite, L. Järnström, K. Koch, Molecular structure of citric acid cross-linked starch films,

Carbohydr. Polym. 96 (2013) 270–276, https://doi.org/10.1016/j.carbpol.2013.03.044.
[27] H. Klaushofer, J. Bleier, Versuche zur Aufklärung der Struktur von Citratstärken, Starch-Starke 35 (1983) 237–242, https://doi.org/10.1002/star.19830350705.
[28] Y. Qin, W. Wang, H. Zhang, Y. Dai, H. Hou, H. Dong, Effects of citric acid on structures and properties of thermoplastic hydroxypropyl amylomaize starch films, Materials 12 (2019) 1–13, https://doi.org/10.3390/ma12091565.
[29] Z. Wu, J. Wu, T. Peng, Y. Li, D. Lin, B. Xing, C. Li, Y. Yang, L. Yang, L. Zhang, R. Ma, W. Wu, X. Lv, J. Dai, G. Han, Preparation and application of starch/polyvinyl alcohol/citric acid ternary blend antimicrobial functional food packaging films, Polymers 9 (2017) 1–19, https://doi.org/10.3390/polym9030102.
[30] R. Shi, J. Bi, Z. Zhang, A. Zhu, D. Chen, X. Zhou, L. Zhang, W. Tian, The effect of citric acid on the structural properties and cytotoxicity of the polyvinyl alcohol/starch films when molding at high temperature, Carbohydr. Polym. 74 (2008) 763–770, https://doi.org/10.1016/j.carbpol.2008.04.045.
[31] J. Li, H. He, He Zhang, M. Xu, Q. Gu, Z. Zhu, Preparation of thermoplastic starch with comprehensive performance plasticized by citric acid, 2022, https://doi.org/10.1002/app.52401.
[32] J.J.M. Halpern, R. Urbanski, A.A.K.A. Weinstock, D.D.F.D. Iwig, R.R.T. Mathers, H. H.A. von Recum, A biodegradable thermoset polymer made by esterification of citric acid and glycerol, J. Biomed. Mater. Res. A 102 (2014) 1467–1477, https://doi.org/10.1002/jbm.a.34821.
[33] J.A. Mariano-Torres, A. López-Marure, M.Á. Domiguez-Sánchez, Synthesis and characterization of polymers based on citric acid and glycerol: its application in non-biodegradable polymers, Dyna 82 (2014) 53–59.
[34] D. Pramanick, T.T. Ray, Synthesis and biodegradation of copolyesters from citric acid and glycerol, Polym. Bull. 19 (1988) 365–370, https://doi.org/10.1007/BF00263938.
[35] M. Adeli, B. Rasoulian, F. Saadatmehr, F. Zabihi, Hyperbranched poly(citric acid) and its application as anticancer drug delivery system, J. Appl. Polym. Sci. 129 (2013) 3665–3671, https://doi.org/10.1002/app.39028.
[36] D.S. Franklin, S. Guhanathan, Investigation of citric acid-glycerol based pH-sensitive biopolymeric hydrogels for dye removal applications: a green approach, Ecotoxicol. Environ. Saf. 121 (2015) 80–86, https://doi.org/10.1016/j.ecoenv.2015.05.003.
[37] M.A. Da Silva, M.G.A. Vieira, A.C.G. Maçumoto, M.M. Beppu, Polyvinylchloride (PVC) and natural rubber films plasticized with a natural polymeric plasticizer obtained through polyesterification of rice fatty acid, Polym. Test. 30 (2011) 478–484, https://doi.org/10.1016/j.polymertesting.2011.03.008.
[38] A. Sinisi, M. Degli Esposti, M. Toselli, D. Morselli, P. Fabbri, Biobased ketal-diester additives derived from levulinic acid: synthesis and effect on the thermal stability and thermo-mechanical properties of poly(vinyl chloride), ACS Sustain. Chem. Eng. 7 (2019) 13920–13931, https://doi.org/10.1021/acssuschemeng.9b02177.
[39] W. Xuan, M. Hakkarainen, K. Odelius, Levulinic acid as a versatile building block for plasticizer design, ACS Sustain. Chem. Eng. 7 (2019) 12552–12562, https://doi.org/10.1021/acssuschemeng.9b02439.
[40] E.J.M. De Paiva, S. Sterchele, M.L. Corazza, D.Y. Murzin, F. Wypych, T. Salmi, Esterification of fatty acids with ethanol over layered zinc laurate and zinc stearate - kinetic modeling, Fuel. 153 (2015) 445–454, https://doi.org/10.1016/j.fuel.2015.03.021.
[41] Y. Wang, J. You, B. Liu, Preparation of mesoporous silica supported sulfonic acid and evaluation of the catalyst in esterification reactions, React. Kinet. Mech. Catal. 128 (2019) 493–505, https://doi.org/10.1007/s11144-019-01645-2.
[42] M. de S. Gomes, M.R.D. Santos, A.B. Salviano, F.G. Mendonça, I.R.S. Menezes, M. Jurisch, G.D. Rodrigues, R. Augusti, P.S. Martins, R.M. Lago, Biphasic reaction of glycerol and oleic acid: byproducts formation and phase transfer autocatalytic effect, Catal. Today 344 (2020) 227–233, https://doi.org/10.1016/j.cattod.2019.02.011.
[43] D.H. Wu, A. Chen, C.S.C.S. Johnson, An improved diffusion-ordered spectroscopy experiment incorporating bipolar-gradient pulses, J. Magn. Reson. Ser. A 115 (1995) 260–264, https://doi.org/10.1006/jmra.1995.1176.
[44] D. Sinnaeve, The Stejskal-Tanner equation generalized for any gradient shape-an overview of most pulse sequences measuring free diffusion, Concepts Magn. Reson. A 40 (2012) 39–65, https://doi.org/10.1002/cmr.a.
[45] I. Fernández, F.M. Arrabal-Campos, L.M. Aguilera-Saéz, Algebraic reconstruction technique for diffusion NMR experiments. Application to the molecular weight prediction of polymers, J. Phys. Chem. A 123 (2019) 943–950, https://doi.org/10.1021/acs.jpca.8b08584.
[46] F.M. Arrabal-Campos, P. Oña-Burgos, I. Fernández, Molecular weight prediction with no dependence on solvent viscosity. A quantitative pulse field gradient diffusion NMR approach, Polym. Chem. 7 (2016) 4326–4329, https://doi.org/10.1039/c6py00691d.
[47] M.D. Eaton, D. Domene-López, Q. Wang, M.G. Montalbán, I. Martin-Gullon, K. R. Shull, I. Martin-Gullon, K.R. Shull, Exploring the effect of humidity on thermoplastic starch films using the quartz crystal microbalance, Carbohydr. Polym. 261 (2021), 117727, https://doi.org/10.1016/j.carbpol.2021.117727.
[48] A. Marcilla, S. García, J.C. García-Quesada, Study of the migration of PVC plasticizers, J. Anal. Appl. Pyrolysis 71 (2004) 457–463, https://doi.org/10.1016/S0165-2370(03)00131-1.
[49] ASTM D882-12, Standard Test Method for Tensile Properties of Thin Plastic Sheeting, ASTM Int., West Conshohocken, PA, USA, 2012, https://doi.org/10.1520/D0882-12. Available Online Https//Www.Astm.Org/DATABASE.CART/HISTORICAL/ D882-02.Htm (Accessed 28 March 2018). (n.d.).
[50] I. Mamajanov, M.P. Callahan, J.P. Dworkin, G.D. Cody, Prebiotic alternatives to proteins: structure and function of hyperbranched polyesters, Orig. Life Evol. Biosph. 45 (2015) 123–137, https://doi.org/10.1007/s11084-015-9430-9.
[51] A. Gadomska-Gajadhur, Biobased poly (glycerol citrate) synthesis optimization via design of experiments, Polym. Adv. Technol. 32 (2021) 3982–3994, https://doi.org/10.1002/pat.5498.
[52] I. Mamajanov, Wet-dry cycling delays the gelation of hyperbranched polyesters: implications to the origin of life, Life. 9 (2019) 56, https://doi.org/10.3390/life9030056.
[53] S. Viamonte-Aristizábal, A. García-Sancho, F.M.A. Campos, J.A. Martínez-Lao, I. Fernández, Synthesis of high molecular weight L-polylactic acid (PLA) by reactive extrusion at a pilot plant scale: influence of 1,12-dodecanediol and di (trimethylol propane) as initiators, Eur. Polym. J. 161 (2021), 110818, https://doi.org/10.1016/j.eurpolymj.2021.110818.
[54] S. Dworakowska, W. Kasprzyk, S. Bednarz, D. Bogdał, Polyesters from renewable sources, in: 15th Int. Electron. Conf. Synth. Org. Chem, 2011, https://doi.org/10.3390/ecsoc-15-00654.
[55] I. Ekaette, M.D.A. Saldaña, Ultrasound-assisted modification of rutin to nanocrystals and its application in barley starch pyrodextrinization, Food Chem. 344 (2021), 128626, https://doi.org/10.1016/j.foodchem.2020.128626.
[56] K.R. Terpstra, A.J.J. Woortman, J.C.P. Hopman, Yellow dextrins: evaluating changes in structure and colour during processing, Starch/Staerke. 62 (2010) 449–457, https://doi.org/10.1002/star.200900254.
[57] R. Shi, Z. Zhang, Q. Liu, Y. Han, L. Zhang, D. Chen, W. Tian, Characterization of citric acid/glycerol co-plasticized thermoplastic starch prepared by melt blending, Carbohydr. Polym. 69 (2007) 748–755, https://doi.org/10.1016/j.carbpol.2007.02.010.
[58] E. Olsson, M.S. Hedenqvist, C. Johansson, L. Järnström, Influence of citric acid and curing on moisture sorption, diffusion and permeability of starch films, Carbohydr. Polym. 94 (2013) 765–772, https://doi.org/10.1016/j.carbpol.2013.02.006.
[59] C. Li, Y. Hu, Effects of acid hydrolysis on the evolution of starch fine molecular structures and gelatinization properties, Food Chem. 353 (2021), 129449, https://doi.org/10.1016/j.foodchem.2021.129449.
[60] Y. Jiugao, W. Ning, M. Xiaofei, The effects of citric acid on the properties of thermoplastic starch plasticized by glycerol, Starch/Staerke. 57 (2005) 494–504, https://doi.org/10.1002/star.200500423.
[61] M. Zdanowicz, R. Jędrzejewski, R. Pilawka, Deep eutectic solvents as simultaneous plasticizing and crosslinking agents for starch, Microvasc. Res. 129 (2019) 1040–1046, https://doi.org/10.1016/j.mvr.2017.09.004.
[62] K. Trinath, K. Sandeepkumar, N. Devarakonda, V. Karthik, Development and characterization of biodegradable blending starch/PVA films theoretical and experimental comparison, IOP Conf. Ser. Mater. Sci. Eng. 402 (2018), https://doi.org/10.1088/1757-899X/402/1/012129.
[63] A. Vinod, Y. Gowda, S. Krishnasamy, M.R. Sanjay, Thermal properties of hybrid natural fiber-reinforced thermoplastic composites, in: Nat. Fiber-reinforced Compos. Therm. Prop. Appl, 2022, pp. 17–30, https://doi.org/10.1002/9783527831562.ch2.
[64] D.D.D. Galusek, S. Reschke, R. Riedel, W. Dreßler, P. Šajgalík, Z. Lenčéš, J. Majling, W. Dreûler, In-situ carbon content adjustment in polysilazane derived amorphous SiCN bulk ceramics, J. Eur. Ceram. Soc. 19 (1999) 1911–1921, https://doi.org/10.1007/bf00882548.
[65] H.D. Özeren, R.T. Olsson, F. Nilsson, M.S. Hedenqvist, Prediction of plasticization in a real biopolymer system (starch) using molecular dynamics simulations, Mater. Des. 187 (2020), 108387, https://doi.org/10.1016/j.matdes.2019.108387.
[66] C.M. Jaramillo, P. González Seligra, S. Goyanes, C. Bernal, L. Famá, Biofilms based on cassava starch containing extract of yerba mate as antioxidant and plasticizer, Starch/Staerke. 67 (2015) 780–789, https://doi.org/10.1002/star.201500033.